

Dynamic clonal progression in xenografts of acute lymphoblastic leukemia with intrachromosomal amplification of chromosome 21

Paul. B. Sinclair,¹ Helen H. Blair,¹ Sarra L. Ryan,¹ Lars Buechler,¹ Joanna Cheng,¹ Jake Clayton,¹ Rebecca Hanna,¹ Shaun Hollern,¹ Zoe Hawking,¹ Matthew Bashton,¹ Claire J. Schwab,¹ Lisa Jones,¹ Lisa J. Russell,¹ Helen Marr,¹ Peter Carey,² Christina Halsey,³ Olaf Heidenreich,¹ Anthony V. Moorman¹ and Christine J. Harrison¹

¹Wolfson Childhood Cancer Research Centre, Northern Institute for Cancer Research, Newcastle University, Newcastle-upon-Tyne; ²Department of Clinical Haematology, Royal Victoria Infirmary, Newcastle-upon-Tyne and ³Wolfson Wohl Cancer Research Centre, Institute of Cancer Sciences, University of Glasgow, UK

©2018 Ferrata Storti Foundation. This is an open-access paper. doi:10.3324/haematol.2017.172304

Received: May 15, 2017.

Accepted: February 8, 2018.

Pre-published: February 15, 2018.

Correspondence: christine.harrison@newcastle.ac.uk

Supplementary methods

Determination of xenograft experimental end points. Mice were checked daily for signs of ill health and routinely weighed once a week or more often if indicated. Mice were culled at end stage disease as defined by; weight gain of >20%, weight loss reaching 20% at any time or >10% maintained for 72 hours compared with weight at the start of the experiment, starey coat, porphyrin staining of eyes and nose or sunken eyes, persistent skin tenting, immobility, unresponsive or very aggressive behaviour, loss of upright stance, laboured respiration, blood staining or other discharge, signs of anaemia including extreme paleness of feet, tail and ears.

Immunophenotyping of xenografts cells. Proportions of human and mouse cells were determined by flow cytometry using anti-human CD10 FITC or CD19 PE in combination with anti-murine-CD45, PE-Cy7 and anti-TER119 PE-Cy7, as previously described.(1) Selected xenografts were further characterised using a panel of anti-human CD19-APC, CD10-PE, CD34-Cy5.5 and CD38-FITC together with anti-mouse CD45-Cy7-A. Cells were initially gated on a lymphocyte population defined by forward and side scatter and on the anti-mouse CD45 negative population. For each sample, identical markers were used to divide the gated cells into human CD19, CD10, CD45 and CD38 negative and positive populations based on median fluorescence intensity (MFI) of the unstained cells. MFI and % positive cells (supplementary table 5) refer to the total gated population with the exception of a minority of samples where the proportion of cells staining positively for mouse CD45 was high and a significant proportion of gated cells, negative for all human markers, was assumed to be of mouse origin and gated out. All antibodies were obtained from BD Biosciences (Oxford, UK) and stained cells were analysed with a BD FACSCanto II cell analyser and processed with FlowJo (Oregon, USA) software .

Lentiviral transduction, In-vitro culture and in-vitro, in-vivo and ex-vivo imaging of xenograft cells. SLIEW lentivirus was produced as previously described(1) with the modification that HEK293FT cells (Thermo Fisher Scientific) and EndoFectin (GeneCopoeia) transfection reagent were used. Lentiviral stocks were concentrated by ultracentrifugation for 2 hours at an RCF of 83018 and re-suspended in Serum free expansion medium (SFEM) (Stemcell Technologies) supplemented with 10% FCS before titrating in 293FT cells. For each patient analysed, 1.2×10^7 xenograft cells in SFEM supplemented with 10% FCS and 10ng/ml IL-7, were transduced at a multiplicity of infection of 1.0 in delta T25 tissue culture flasks. Following overnight incubation medium was replaced and approximately 72 hours after transduction 0.5×10^6 cells were analysed for EGFP expression by FACS, 1.5×10^6 cells were transplanted into each of two NSG mice and 6×10^6 cells were re-suspended in α MEM with 10% FCS for in-vitro co-culture. Co-cultures were established by plating 2×10^6 transduced xenograft cells in

1ml of medium on MS-5 cells (DSMZ # ACC441) (83,000 cells plated /well in 12 well plates) that had been irradiated with 50 Gy 24hrs after plating. EGFP expression of co-cultured cells was assessed using an EVOS fluorescent inverted microscope (Life technologies). 2D and 3D bioluminescent whole body imaging of mice transplanted with transduced xenograft cells was performed with an IVIS Spectrum (Caliper Life Sciences, Hopkington, MA, USA) 10 minutes after intraperitoneal injection of 100ul of D-luciferin (30mg/ml, VivoGlo, Promega). Immediately following final whole body imaging mice were killed and organs dissected and imaged ex-vivo. Quantification of luminescent signals and 3D reconstructions were performed using Living image version 4.3.1 software (Caliper Life Sciences). The proportion of leukaemia cells expressing SLIEW in spleen preparations was measured by immunostaining and FACS by determining numbers of EGFP+ve cells in the human CD19+ve and / or CD10+ve, murine CD45 / TER119 –ve population.

Histopathology.

After transfer to 10% neutral buffered formalin immediately after dissection, tibias and sternums were decalcified, paraffin embedded, sectioned and stained with haematoxylin and eosin (H&E) or human antibodies, according to standard histopathological techniques, by the department of Cellular Pathology, Newcastle upon Tyne Hospitals NHS Foundation Trust. Mouse heads preserved in formalin were sectioned and stained as previously described.(2)

Transmission Electron Microscopy (TEM). TEM was performed by the Electron Microscopy Unit, Faculty of Medical Sciences, Newcastle University. Small trephines of bone were fixed in 5% glutaraldehyde in 3% PFA in phosphate buffer overnight. Samples were then rinsed in phosphate buffer before being placed in EDTA for a minimum of 24hrs at 40°C. After rinsing in phosphate buffer the samples were placed in 1% osmium tetroxide for 2hrs at RT. They were then rinsed in buffer, dehydrated through a graded series of acetone and embedded in TAAB epoxy resin (medium). After polymerisation at 60°C the samples were sectioned on an ultramicrotome and ultrathin sections (70nm) were picked up on copper grids, stained with uranyl acetate and lead citrate and viewed on a Philips CM100 TEM at 100kV.

RNA Sequencing.

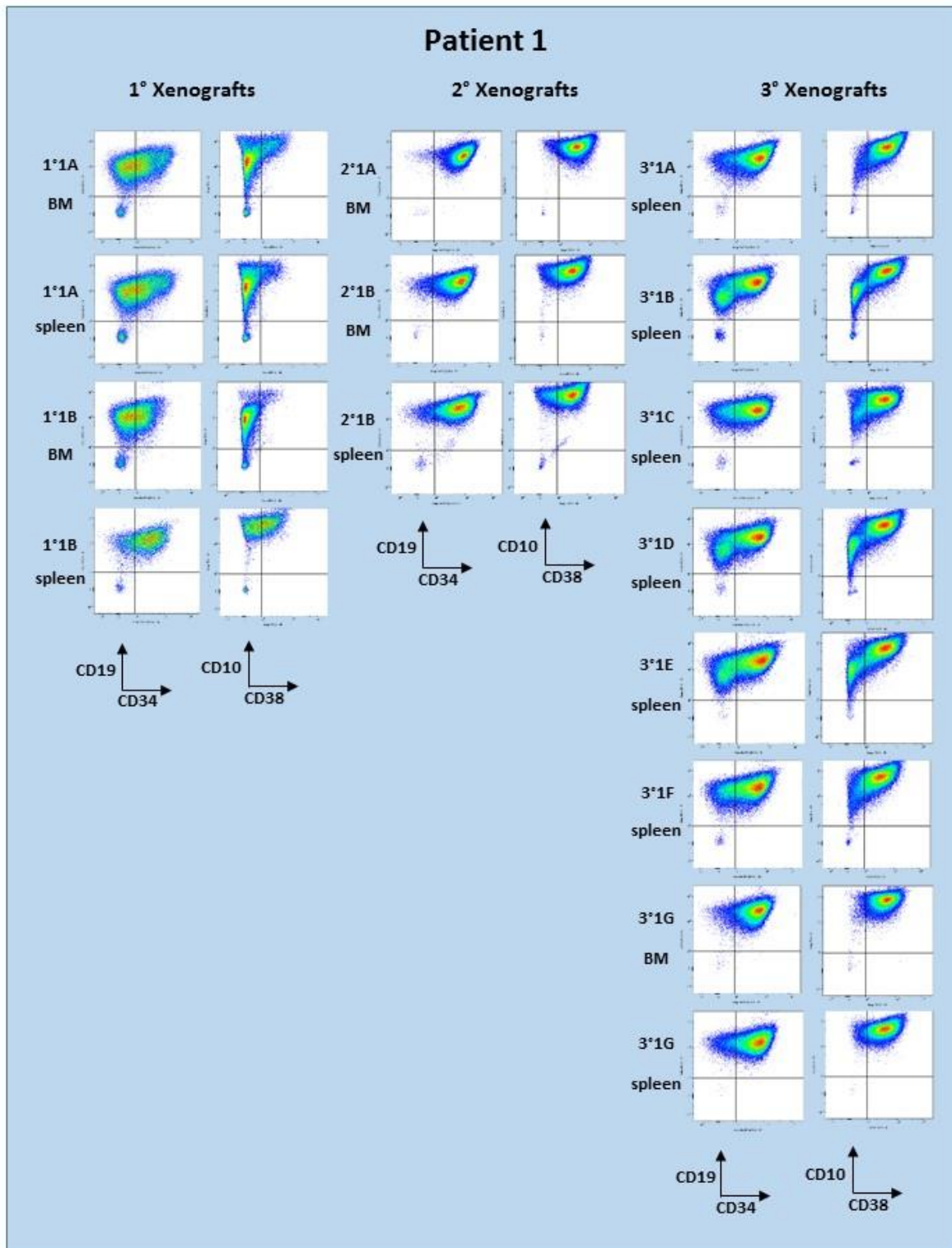
RNA was extracted from cells isolated from xenograft spleens and purified over Ficol using an RNeasy kit (Qiagen). Illumina RNA sequencing was performed by Aros Applied Biotechnology, Eurofins Genomics Group, Aarhus, DK.

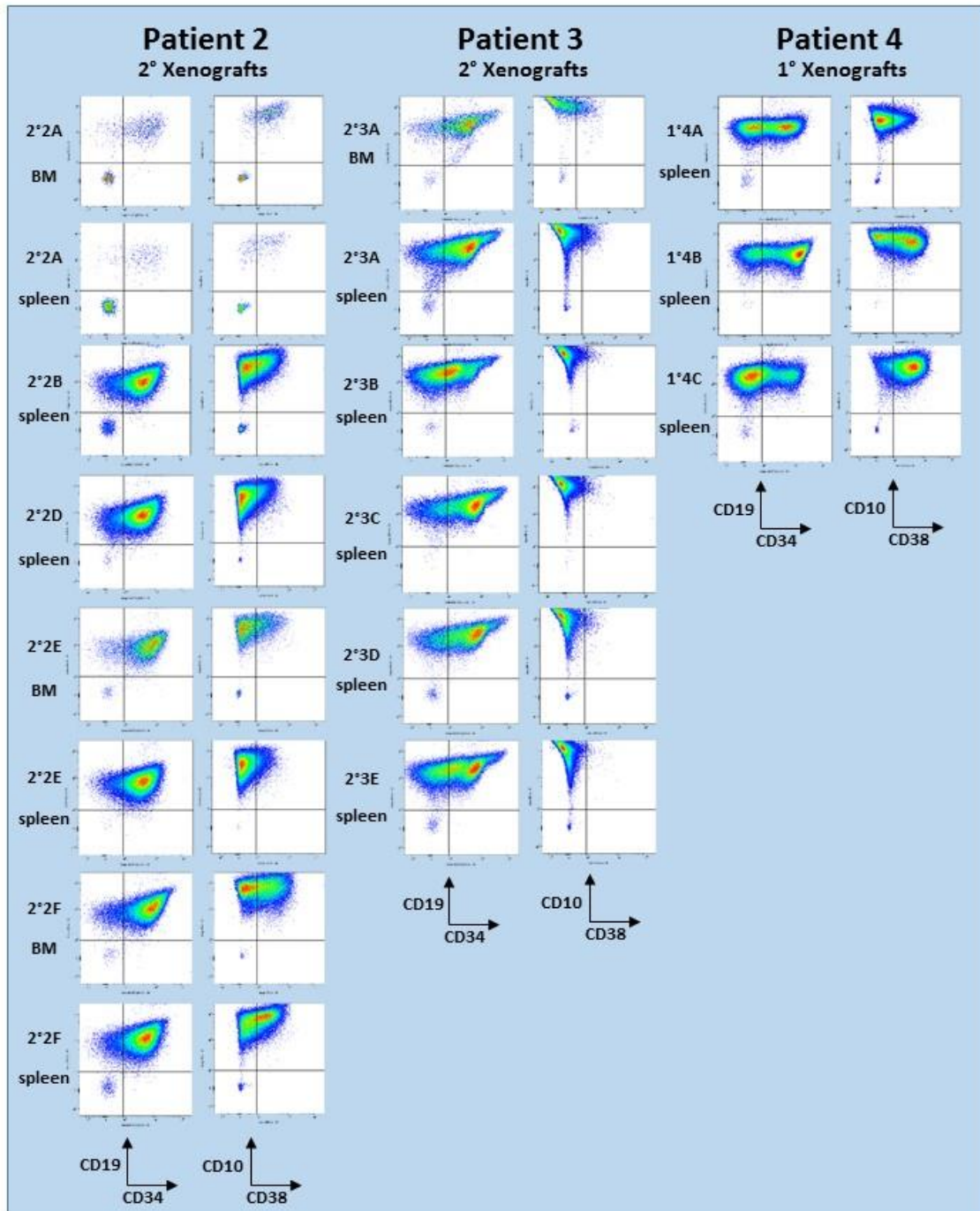
Analysis of RAS pathway mutations. Whole exome sequencing (WES) was performed on selected xenografts derived from patient 1 using library preparation and sequencing techniques as previously

described(3). To filter mouse sequences from xenograft samples, the programme, Xenome v 1.0.1, was used to simultaneously align reads to version GRCh38 and hg19 of the mouse and human genomes, respectively(4). Default settings of xenome index and classify were used to designate reads as of human or mouse origin, ambiguous, both or neither, with only unambiguous human reads used for subsequent analysis. Reads were aligned using Burrows-Wheeler Aligner (BWA) version 0.7.12.(5, 6) and MuTect1.7 (7) was used for calling somatic single nucleotide variants (SNVs) following Broad Best practices(8, 9). Calls were derived from jointly realigned and recalibrated tumour normal (patient remission sample) BAM files and annotated with ENSEMBL Variant Effect Predictor (VEP) version 83(10). Patient BAM files were re-analysed manually in Integrated Genome Viewer(11) to assess levels of SNV affecting the RAS pathway, predicted to have an oncogenic role (mutations located within coding regions and predicted to affect protein function using SIFT, Polyphen2 and Mutation Taster) and identified by WES in xenografts but not previously in the patient (KRAS, chr12:25380276, T->A; NRAS, chr1:115258744, C->T).

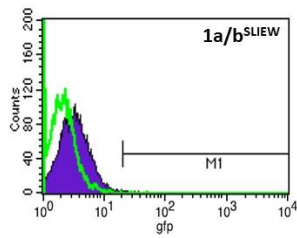
To validate clonal SNV affecting *NF1*, *NRAS* and *KRAS* and extend analysis to remaining patient 1 xenografts, affected exons were amplified and analysed by sanger-sequencing (Durham Genome Centre, Durham UK). Sequence traces were examined manually using FinchTV (Information Technologies, Inc, MO, USA). Target sequence amplification and Sanger-sequencing was also used to analyse an NRAS mutation in xenografts, previously identified in patient 3. Levels of a *FLT3* 30 nucleotide internal tandem duplication (ITD) identified in patient 5 were assessed in xenografts and a relapse sample using targeted sequencing in combination with electrophoretic analysis of amplicon size using a 2100 Bioanalyzer (Agilent technologies, CA USA). All primer sequences used for exon amplification have been previously published (3).

Supplementary Figures





Supplementary Figure 1. FACS analysis demonstrates immunophenotypic heterogeneity between xenografts. Expression of CD19, CD34, CD10 and CD38 are shown for bone marrow (BM) and / or spleen samples for xenografts from patients 1-4 as indicated. Scales are bi-exponential and units are arbitrary.

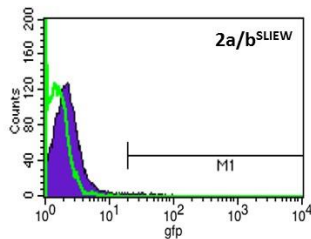
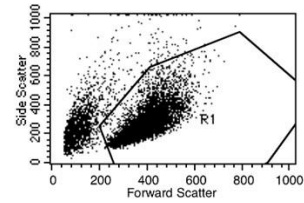


File: control 3.037

% Gated	% Total	Mean	Median
100.00	82.29	2.22	1.95
0.02	0.02	35.60	34.14

File: Sample 3.038

% Gated	% Total	Mean	Median
100.00	81.00	3.57	3.11
0.09	0.07	24.62	22.27

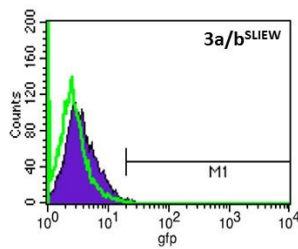
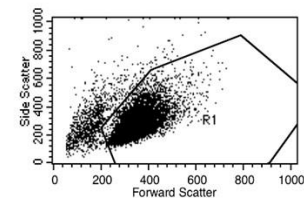


File: control 4.039

% Gated	% Total	Mean	Median
100.00	100.00	1.68	1.43
0.07	0.07	53.04	33.98

File: Sample 4.040

% Gated	% Total	Mean	Median
100.00	87.73	2.47	2.07
0.39	0.34	38.67	31.91

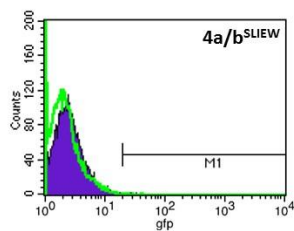
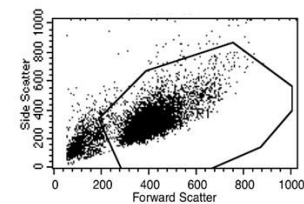


File: control 2.034

% Gated	% Total	Mean	Median
100.00	100.00	3.05	2.48
0.14	0.14	60.19	38.20

File: sample 2.036

% Gated	% Total	Mean	Median
100.00	85.66	4.14	3.34
0.18	0.15	22.47	21.67

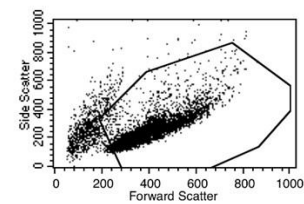


File: control 1.032

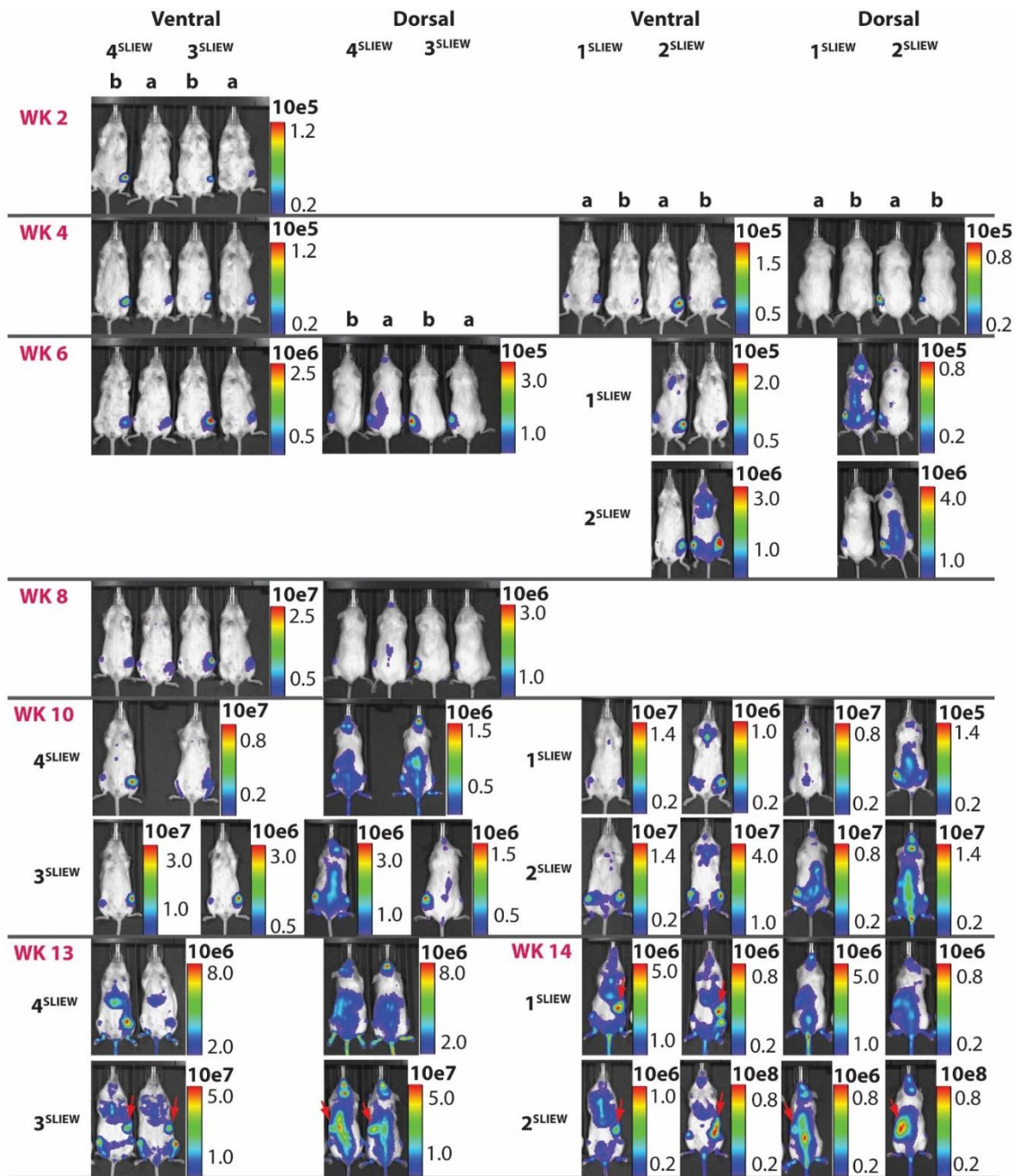
% Gated	% Total	Mean	Median
100.00	90.32	2.20	1.78
0.01	0.01	21.29	21.29

File: Sample 1.033

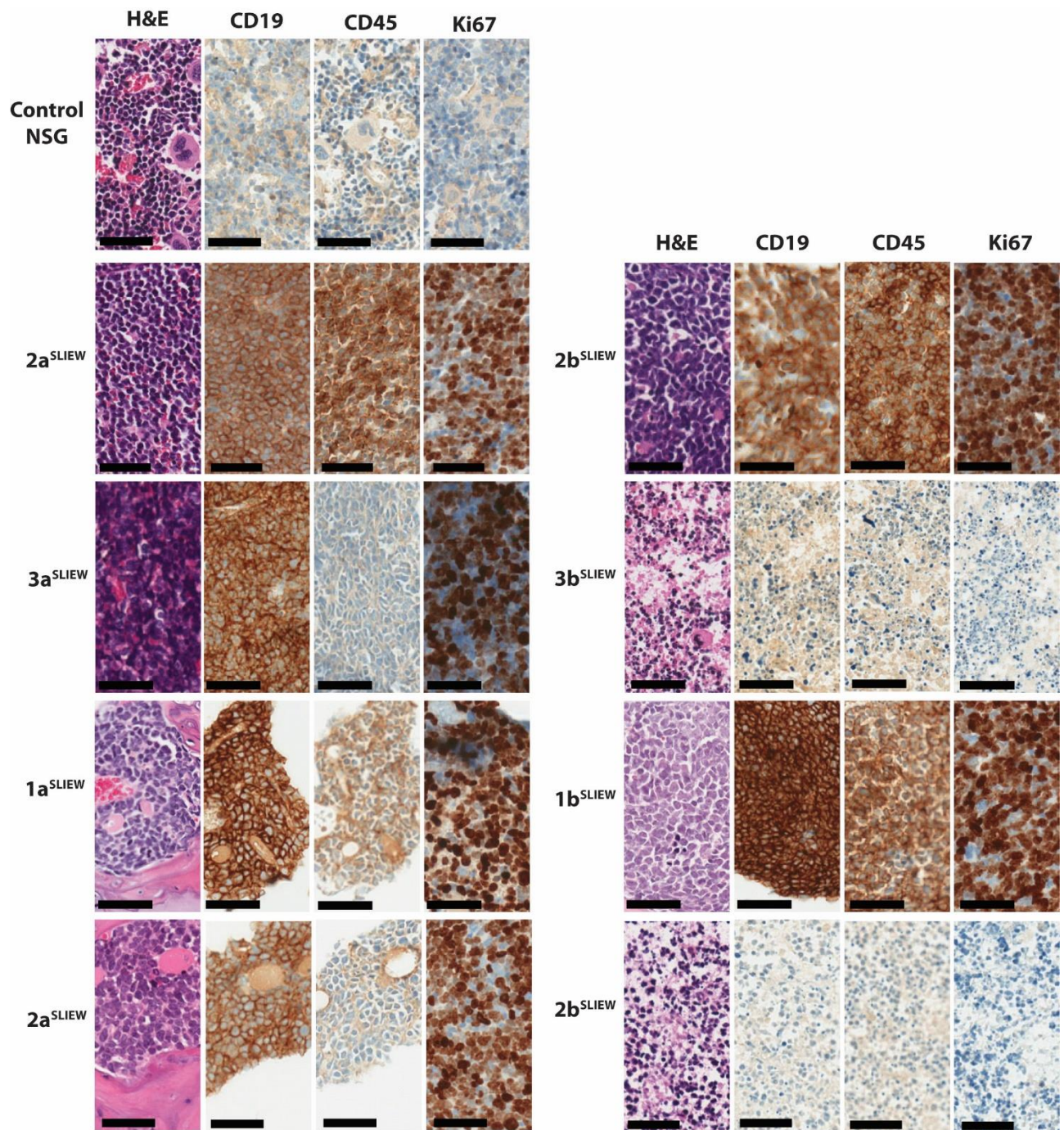
% Gated	% Total	Mean	Median
100.00	88.50	2.68	2.25
0.10	0.09	27.37	26.42



Supplementary figure 2. FACS analysis of iAMP21-ALL cells isolated from xenografts transduced with SLIEW lentivirus prior to transplant. FACS plots showing levels of EGFP expression (arbitrary units) in control (green trace) or transduced cells (purple infill). Live cells were gated on forward and side scatter as shown in the right hand box. In all cases the proportion of cells with GFP levels outside the control range (marker by M1) were less than 1%.

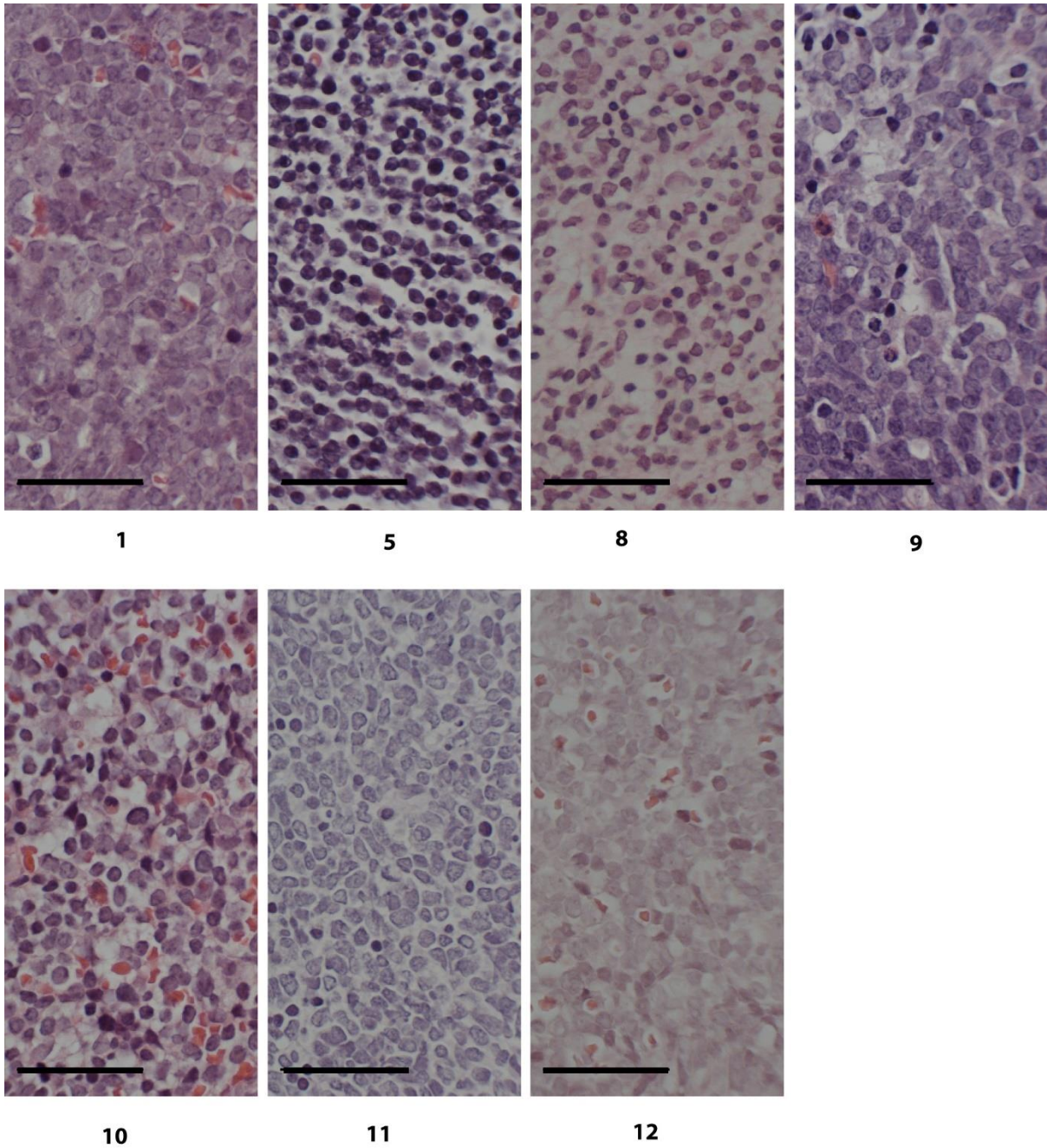


Supplementary Figure 3. Serial bioluminescent imaging of all NSG mice transplanted with pSLIEW transduced iAMP21-ALL xenograft derived cells. Measurement of luciferase activity demonstrates variation in the rate of spread of leukaemia from the site of injection to other bones and organs. Spleen involvement (marked by red arrows) was most obvious in 1a^{SLIEW}, 1b^{SLIEW}, 2a^{SLIEW} and 2b^{SLIEW} but undetectable in 4a/b^{SLIEW}. All captured images are shown. Scale is radiance (p/sec/cm²/sr).

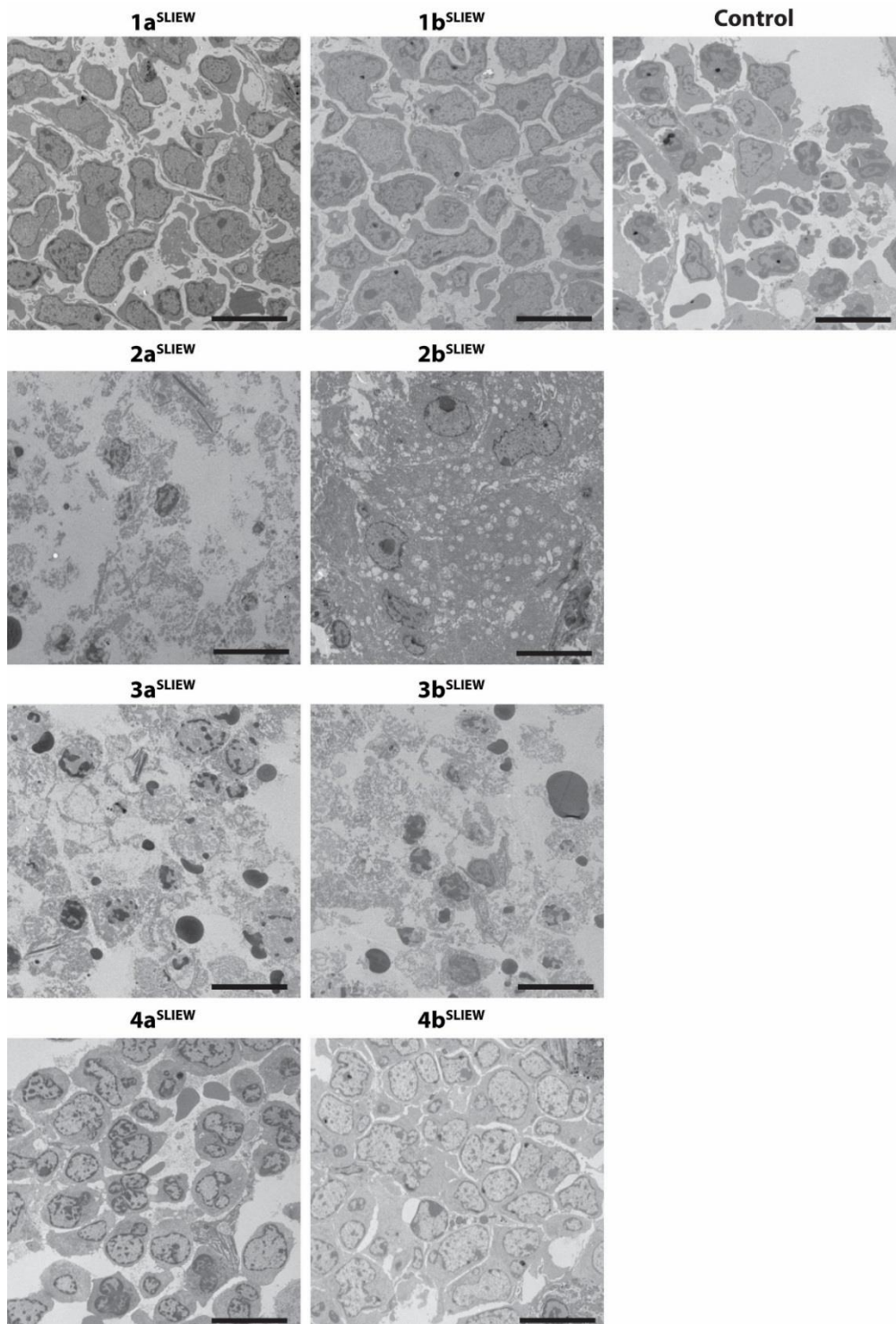


Supplementary Figure 4. Histological sections of control and SLIEW transduced iAMP21-ALL xenograft bone marrows.

Sections of NSG control and xenograft mouse tibias stained with H&E and anti-human CD19, CD45 and Ki67. 4a^{SLIEW}, 4b^{SLIEW}, 3a^{SLIEW}, 1a^{SLIEW}, 1b^{SLIEW} and 2a^{SLIEW} have packed homogeneous cells similar to those seen in iAMP21-ALL patient trephines (Figure 2G and Supplementary Figure 5), that stain positively for human CD19 and Ki67 and for CD45 in 4a^{SLIEW}, 4b^{SLIEW}, 1a^{SLIEW} and 1b^{SLIEW} only (morphology type A). 3b^{SLIEW} and 2b^{SLIEW} show loss of cellularity and evidence for apoptosis and stain negatively for CD19, CD45 and Ki67 (morphology type B). In each case the image shown is representative of all bone marrow in the section analysed. Scale bars are 50µm.

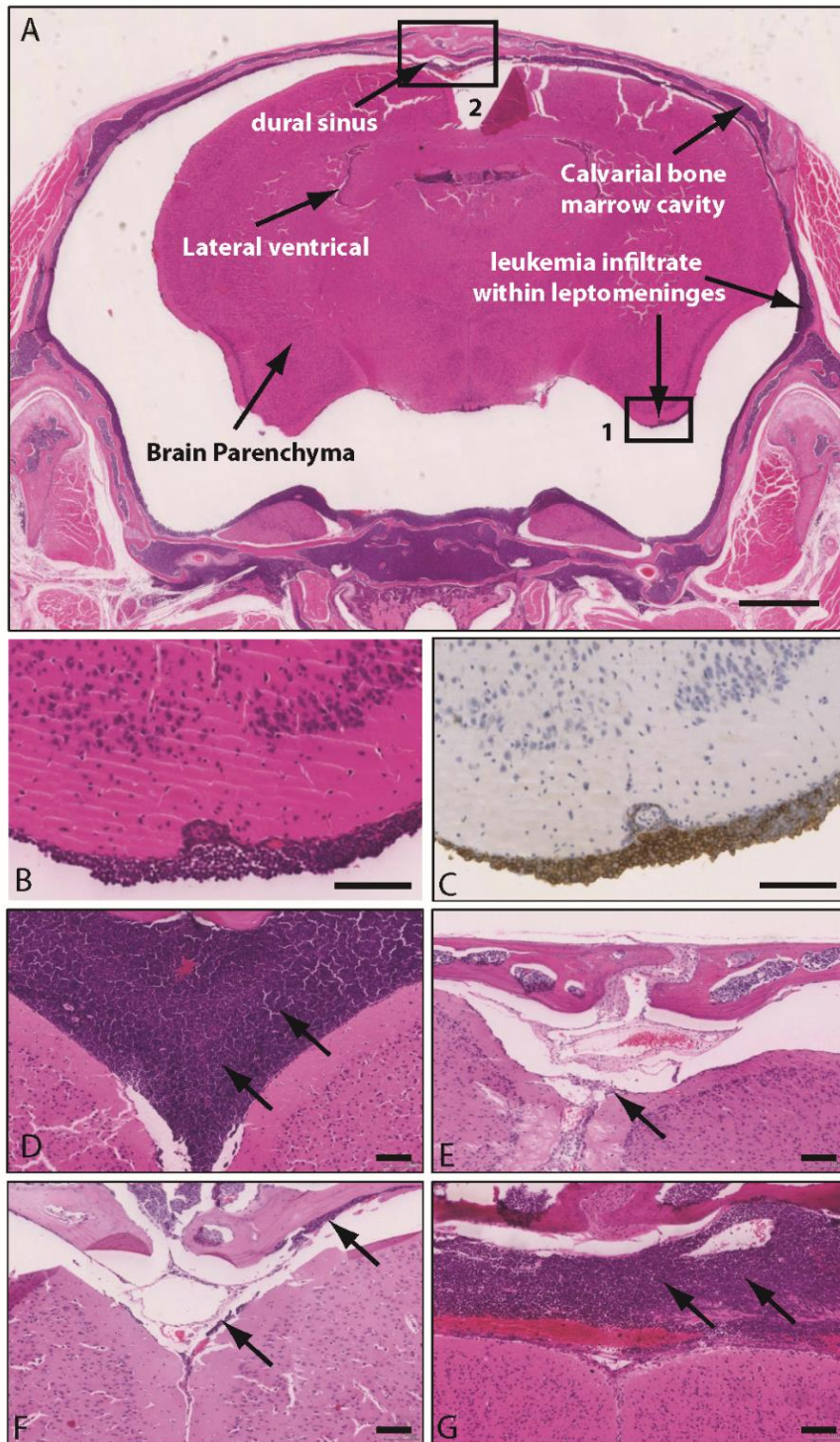


Supplementary Figure 5. iAMP21-ALL patient trephines. H&E stained sections through iAMP21-ALL trephine sections showing morphology similar to that of xenograft type A (Figure 2 and Supplementary Figure 4) with packed homogeneous cells and loss of vasculature and megakaryocytes. Patient karyotypes and demographic details are provided in supplementary table 2. In each case the image shown is representative of all bone marrow in the trephine section. Scale bars are 50 μ m.



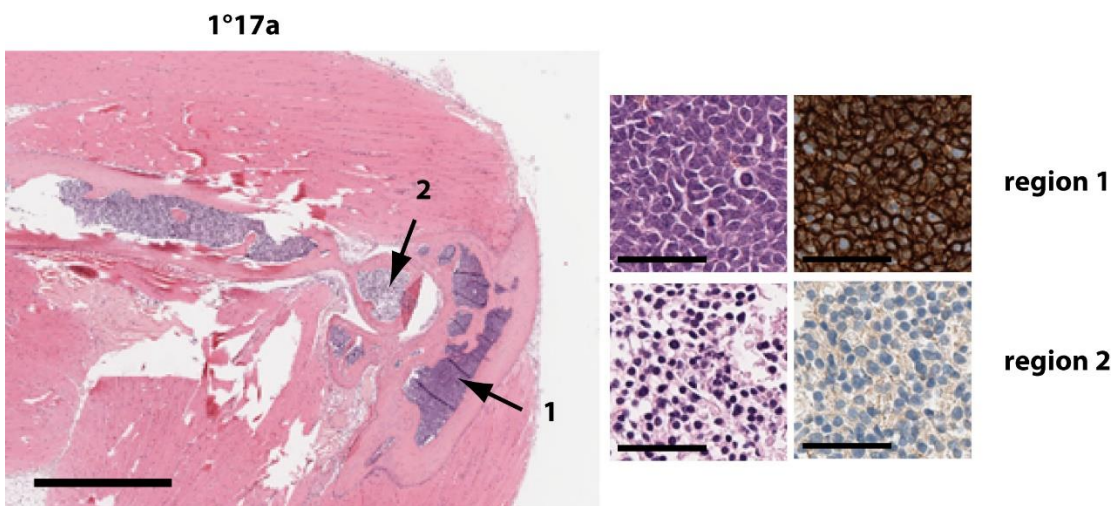
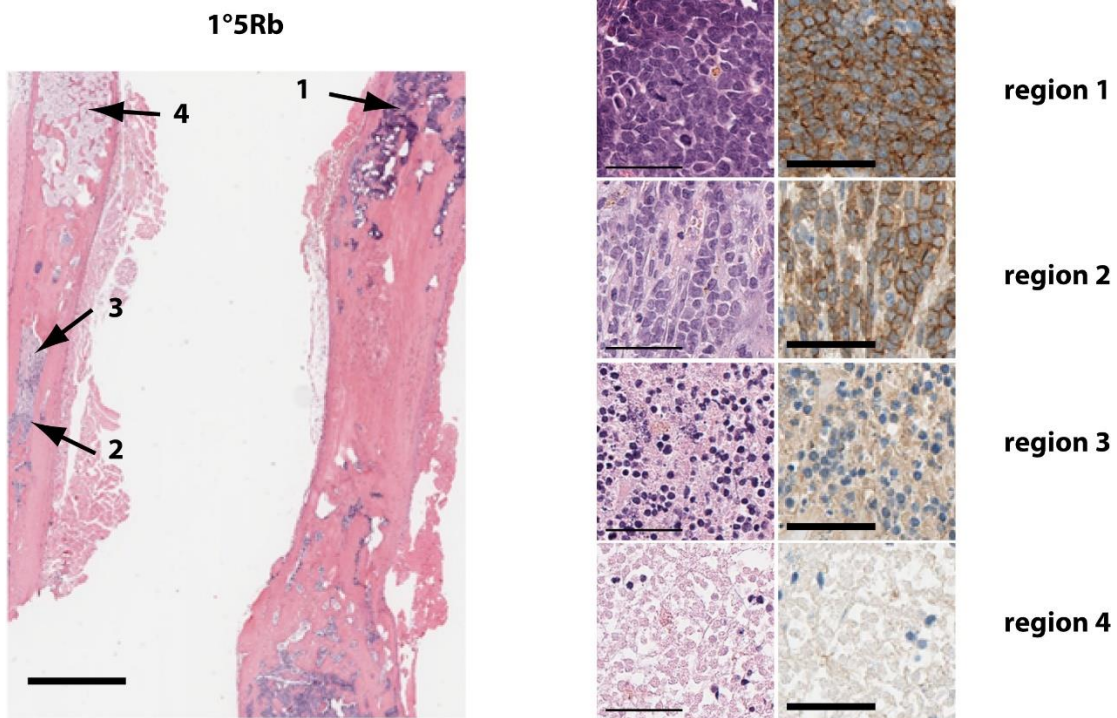
Supplementary Figure 6. Transmission electron microscopy (TEM) of control and SLIEW transduced iAMP21-ALL xenograft bone marrows.

TEM of ultra-thin sections of xenograft bone marrow; 4a^{SLIEW}, 4b^{SLIEW}, 1a^{SLIEW} and 1b^{SLIEW} have homogeneous cells with high nuclear to cytoplasmic ratio (VL morphology), compared with the control section, they lack vascular structures and cellular heterogeneity. 2a^{SLIEW}, 2b^{SLIEW}, 3a^{SLIEW} and 3b^{SLIEW} show loss of cellularity and evidence for apoptosis, such as chromatin clumping and nuclear fragmentation (AP morphology). Each image is representative of 6 regions captured from a single tibia section. Scale bars are 10µm.

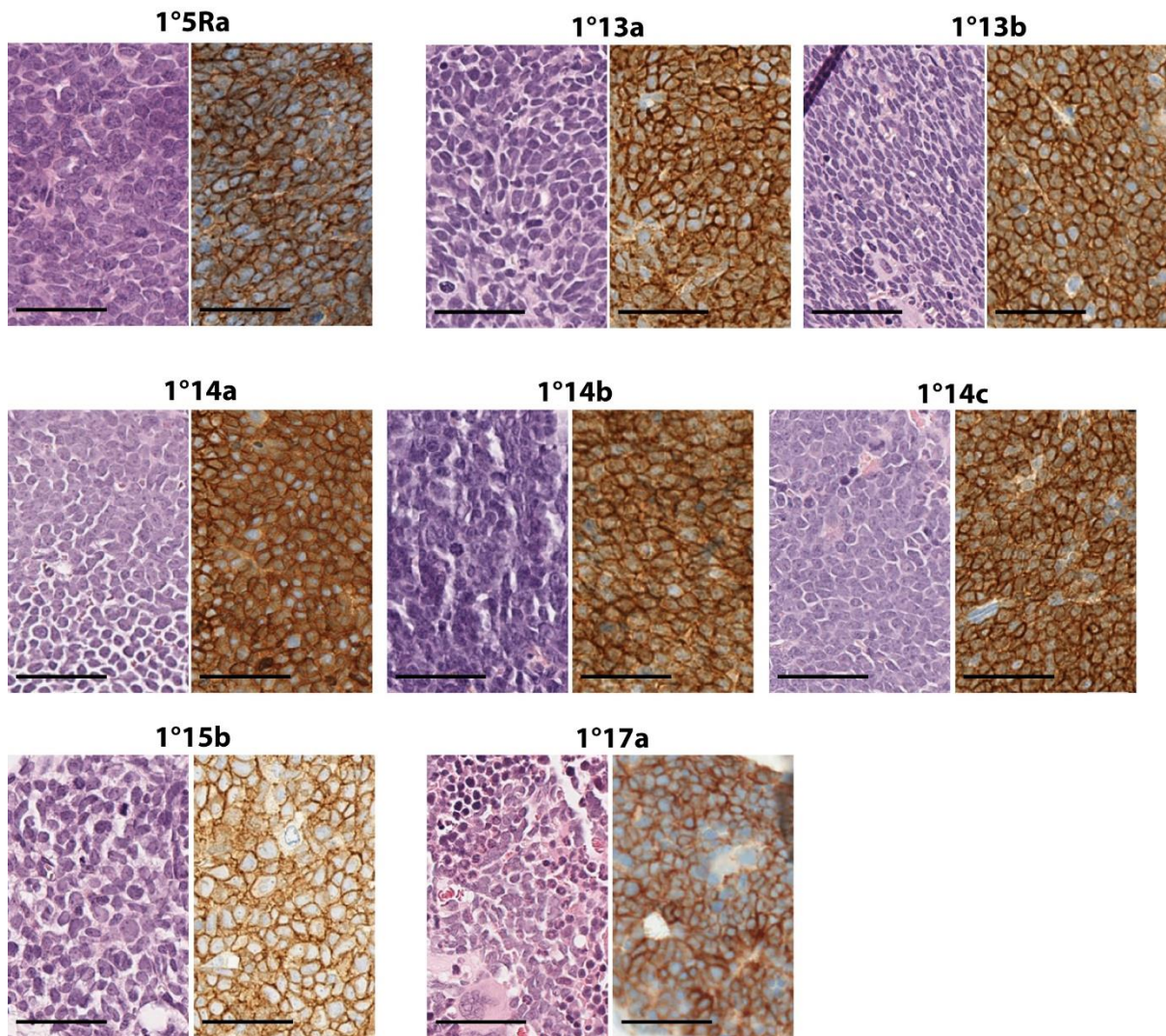


Supplementary Figure 7. SLIEW transduced Xenograft CNS histological sections.

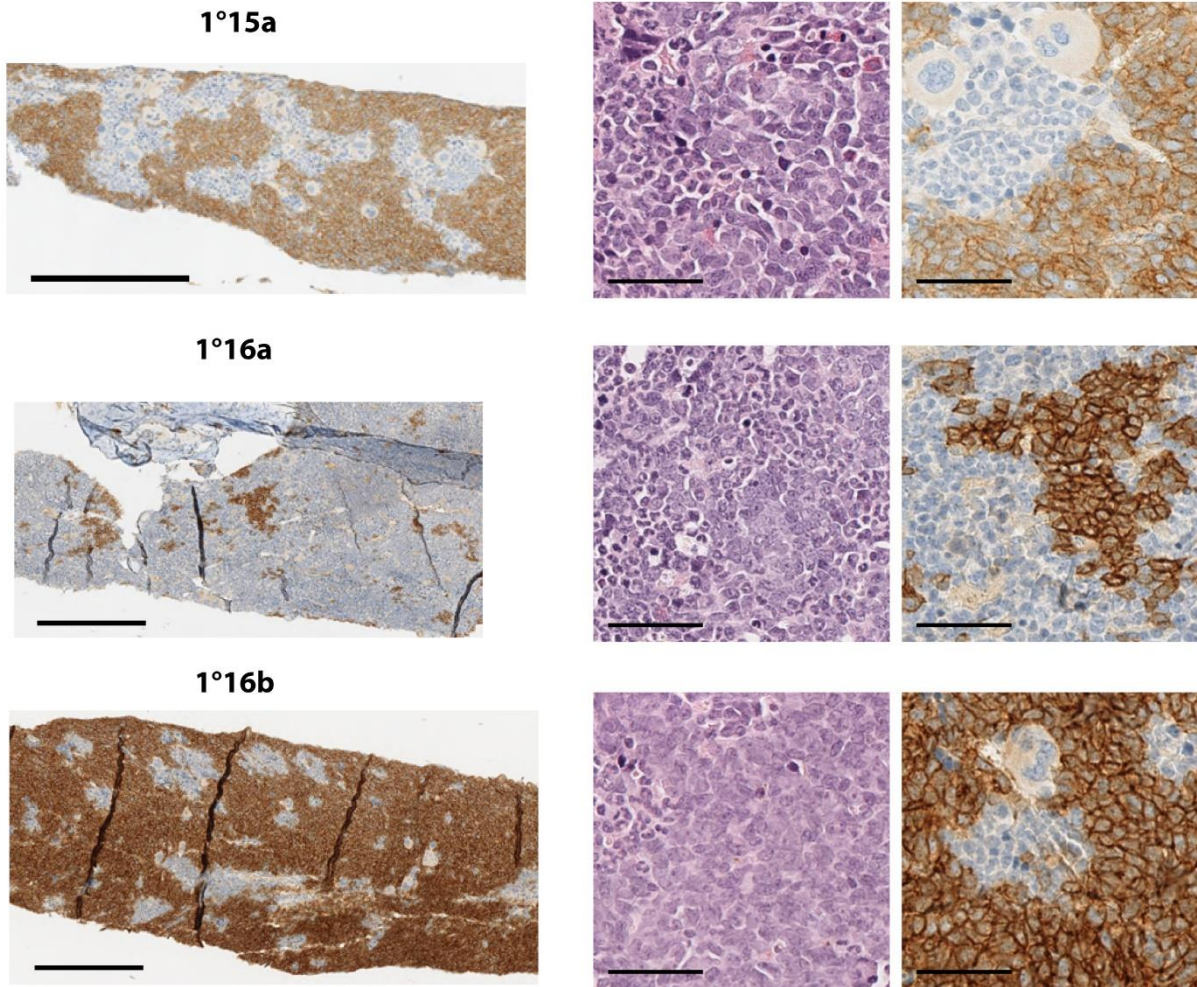
A. H&E stained low powered image of a coronal section through the brain and skull of 1a^{SLIEW} with major structures and areas of leukaemia infiltrate marked with arrows. Scale bar is 1 mm. Leukaemic deposit on the surface of the brain in the region marked in box 1 is shown in detail in **B** (stained with H&E) and in **C** (stained with anti-human CD45). Scale bars are 100µm. **D-G** H&E stained detail of the dural sinus region, marked by box 2 in **A**, showing varying degrees of leukaemic infiltrate of the leptomeninges marked by arrows, in xenografts from; 4b^{SLIEW} (**D**), 2a^{SLIEW} (also representative of 2b^{SLIEW}) (**E**), 3a^{SLIEW} (also representative of 3b^{SLIEW}) (**F**) and 1a^{SLIEW} (also representative of 1b^{SLIEW}) (**G**). Scale bars are 100µm.



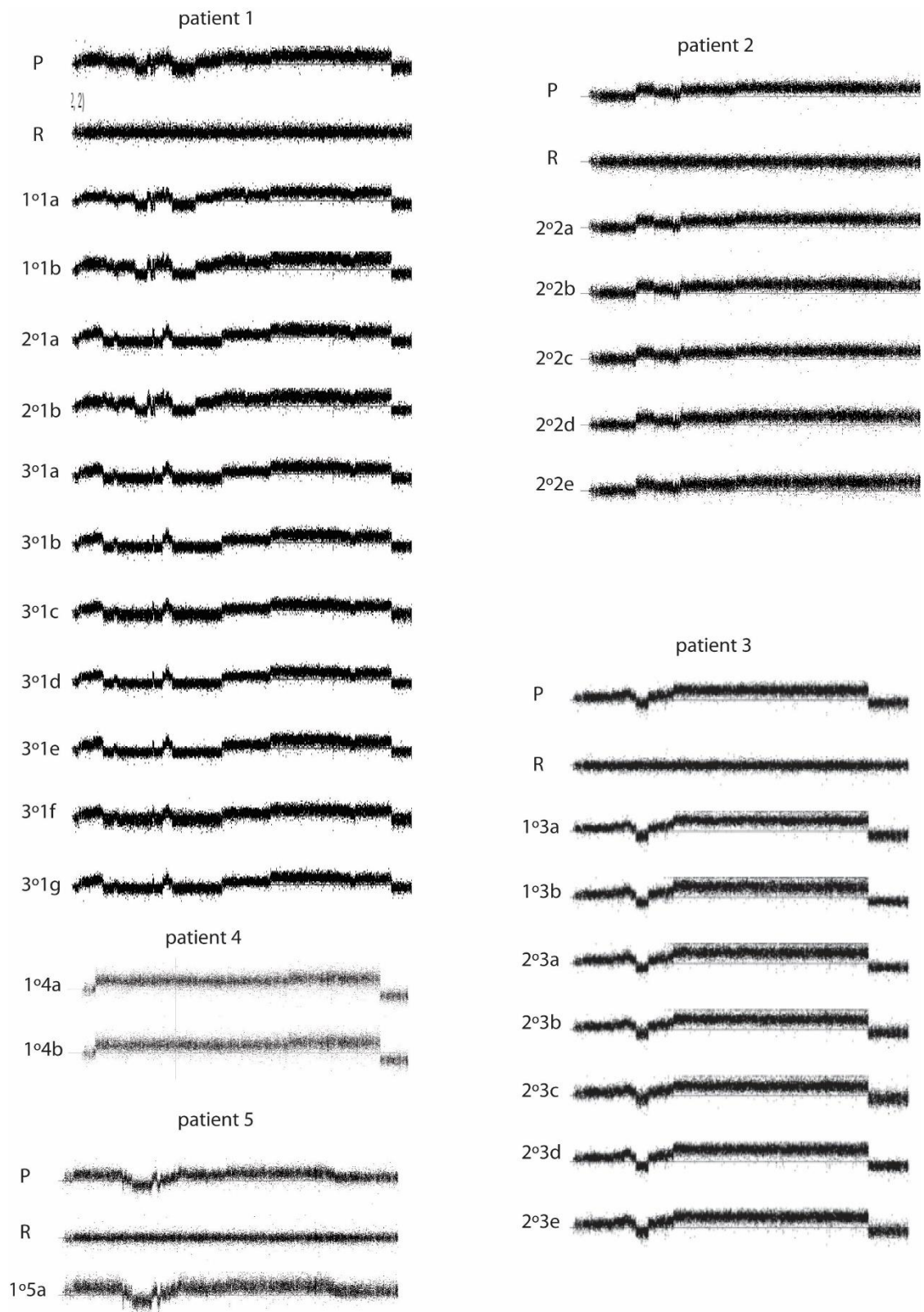
Supplementary figure 8. Histological sections of additional xenografts showing both A and B type morphology. Upper and lower left hand panels show low magnification image of H&E stained sections of fibia and sternum and of the fore limb of xenografts derived from a relapsed iAMP21-ALL (1°5Rb) and a high hyperdiploid ALL respectively (1°17a). Right hand panels show high magnification H&E and human anti-CD19 stained images of regions marked in the left hand panels by arrows. Regions 1 and 2 of the 1°5Rb section and region 1 of the 1°17a section show A-type morphology. Region 3 and 4 of 1°5Rb and region 2 of 1°17a show B type morphology. Scale bars are 1500µm and 50µm for low and high magnification images respectively.



Supplementary Figure 9. Histological sections of additional xenografts showing A type morphology only. High magnification images of bone marrow sections stained with H&E and CD19 taken from tibias, fibias or sternum of additional primografts. The regions shown are representative of all bone marrow observed in a single section of 1 or 2 bones. Scale bars are 50 μ m.



Supplementary Figure 10. Histological sections of additional xenografts showing patches of A-type morphology infiltrating apparently normal mouse bone marrow. Left hand panels show low magnification images of human anti-CD19 stained sections of iAMP21 xenografts showing areas of positively and negatively stained cells. Right hand panels show high magnification H&E and anti-CD19 staining for the same sections. In all three sections infiltrating leukaemia cells are organized into clumps with non-infiltrated areas resembling normal mouse bone marrow. The images shown are representative of a single section of 1 or 2 bones. Scale bars 300 and 50um for low and high magnification images respectively.



Supplementary Figure 11. SNP6.0 chromosome 21 CN profiles for all patient and xenograft samples analysed.

Samples from presentation (P), remission (R) and xenografts. With the exception of patient 1, profiles were indistinguishable between patient leukemia and/or across xenograft samples.

Supplementary Tables

Supplementary Table 1. Karyotypes and demographic details of iAMP21-ALL patient samples used to create xenografts

Patient registration number	ID this study	Presentation (P) /relapse (R)	Karyotype*	Age (years)	Sex	Previously published patient ID	
						A	B
23229	1	P	47,XX,+10,der(21)r(21)(q?)[10]	10	F	437	1
19578	2	P	48,XY,+X,?t(6;20)(p1;q1),?t(7;9)(p1;p2),i(9)(q10),+12,der(21)(q?)[9]	11	M	426	
21567	3	P	52,XX,+9,-12,-12,+7mar[cp4]	8	F	430	14
23317	4	R	45,X,del(X)(q22),del(1)(p13),der(9;17)(q10;q10),del(10)(q22),del(11)(q14),add(21)(q22)[4]/46,idem,+mar[4]	17	F	439	
24259	5	P	46,XX,t(2;16)(p1?2;q2?3),-21,+mar[5]	13	F	447	7
Samples which failed to engraft							
19578**	2	R	Karyotype not available no RUNX1 amplification	11	M	426	45
9028	6	P	46,X,add(X)(q26-q28),?7,der(21)dup(21)(q?)[8]	10	F	511	28
9864	7	P	47,XY,dup(21)(q?),+dup(21)(q?)[6]	10	M	512	18

Age and white blood cell count (WBC) are at diagnosis. *Normal population excluded from abnormal karyotypes. ** Sample was from a case which relapsed in the CNS with no evidence for iAMP21 by interphase FISH of the bone marrow indicating that the blast count was low in this sample. Previously published IDs refer to previous publications; **A** - Harrison *et al* 2014(12) **B** - Ryan *et al* 2016(3).

Supplementary Table 2. Karyotypes and demographic details of iAMP21-ALL with bone marrow trephines used for histological comparison with iAMP21-ALL derived xenografts.

Patient registration number	ID this study	Presentation (P) /relapse (R)	Karyotype**	Age (years)	Sex	Previously published patient ID	
						A	B
23229*	1	P	47,XX,+10,der(21)r(21)(q?)[10]	10	F	437	1
24259*	5	P	46,XX,t(2;16)(p1?2;q2?3),-21,+mar[5]	13	F	447	7
5754	8	P	46,XY,ider(21)(q10)dup(21)(q?)[6]	9	M	478	
21795†	9	P	46,XX[20]	8	F		
23982	10	P	46,XX,add(21)(q2?2)[6]	8	F	444	21
25821	11	P	46,XX,del(7)(q22),del(8)(q22),add(15)(q26),der(21)[cp10]	25	F		
27421†	12	P	N/A	14	F		

Age was at diagnosis. *Patients 1 and 5 were also used to create xenografts. †iAMP21 identified by interphase FISH. **Normal population excluded from abnormal karyotypes. N/A, not available. Previously published IDs refer to previous publications; **A** - Harrison *et al* 2014(12) **B** - Ryan *et al* 2016(3).

Supplementary Table 3. Karyotypes and demographic details of additional B-ALL patient samples used to create xenografts examined histologically.

Patient registration number	ID this study	Genetic subtype /Presentation (P) or relapse (R)	Karyotype**	Age (years)	Sex	Previously published patient ID	
						A	B
22322	12	iAMP21/P	46~47,XX,+?X,add(7)(p22),del(11)(q23),del(13)(q12q14),dup(21)(q22),+r	8	F	433	15
20724*	13	iAMP21/P	46,XY	3	M	429	16
23299	14	iAMP21/P	46,XY,der(1)t(1;13)(q2?5;q12),?del(9)(p2?1),-11,-13,-15,del(16)(q10),-17,-21,+3mar[5]/45,XY,rob(15;21)(q10;q10)?c[5]	10	M	439	43
22340	15	iAMP21/P	46,XX,ider(21)?inv dup(21)(q1q2)[9]	10	F	434	11
24259*	5	iAMP21/R	N/A	13		447	7
10420†	16	ETV6-RUNX1/P	46,XY,del(6)(q13q23),add(8p),der(12)?t(12;22)(p?;q?),+21,-22,der(22)t(?;22)	3	M		
2058	17	Hyperdiploid/P	52,XX,+X,+9,add(9)(p13),+14,+18,+21,+21	4	F		

Age was at diagnosis. *iAMP21 identified by interphase FISH. † ETV6-RUNX1 fusion identified by FISH. ** Normal population excluded from abnormal karyotypes. N/A, not available. Previously published IDs refer to previous publications; **A** - Harrison *et al* 2014(12) **B** - Ryan *et al* 2016(3).

Supplementary Table 4. Details of xenograft generation and ex-vivo analysis of tumour load.

Xenograft id /sex of host	time to cull (weeks)	spleen weight/tumour load**	CD19	CD10	+ve cells Bone marrow	+ve cells Spleen
Patient 1; CD19 92%, CD10 94%, CD34 93%.						
primary mice; 1.6x10 ⁶ cells transplanted / mouse						
1°1a/M	38	1.13g/NA	+ve	+ve	40%	36%
1°1b/M	30	1.43g/NA	+ve	+ve	60%	23%
secondary mice; 2x10 ⁴ 1°1B bone marrow cells transplant / mouse						
2°1a/F	35	0.8g/6x10 ⁸	+ve	+ve	50%	32%
2°1b/F	24	0.33g/NA	+ve	+ve	42%	33%
tertiary mice; 2x10 ⁶ 2°1A spleen cells transplanted / mouse						
3°1a/F	22	1.77g/8.9x10 ⁸	+ve	+ve	Ficol 90%	Ficol 95%
3°1b/F	23	1.6g/1.4x10 ⁹	+ve	+ve	Ficol 98%	Ficol 95%
3°1c/M	28	enlarged*/3.7x10 ⁸	+ve	+ve	NA	Ficol 96%
3°1d/M	28	enlarged*/1.8x10 ⁸	+ve	+ve	NA	Ficol 94%
3°1e/M	27	1.6g/8x10 ⁸	+ve	+ve	92%	Ficol 95%
3°1f/M	27	1.78g/1.5x10 ⁹	+ve	+ve	NA	Ficol 96%
3°1g/M	12	0.66g/2.5x10 ⁹	+ve	+ve	71%	Ficol 99%
Patient 2; CD19 85%, CD10 83%, CD34 80%						
primary mouse 3.3x10 ⁵ transplanted						
1°2a/NA	29	0.285g/NA	+ve	+ve	40%	27%
secondary mice; 1x10 ⁶ 1°2A spleen cells transplanted / mouse						
2°2a/F	8	0.34g/NA	+ve	+ve	6%	5%
2°2b/F	22	0.73g/2.4x10 ⁸	+ve	+ve	18%	Ficol 85%
2°2c/F	22	1.3g/1x10 ⁹	+ve	+ve	NA	NA
2°2d/F	29	1.0g/1.4x10 ⁹	+ve	+ve	NA	Ficol 97%
2°2e/F	29	1.5g/6x10 ⁸	+ve	+ve	NA	NA
2°2f/F	23	1.2g/1.5x10 ⁹	+ve	+ve	51%	Ficol 80%
2°2g/M	25	1.3g/2.5x10 ⁸	+ve	+ve	48%	Ficol 85%
Patient 3; CD19 85%, CD10, 84%, CD34 83%						
primary mice; 1x10 ⁶ cells transplanted / mouse						
1°3a/F	25	enlarged*/NA	+ve	+ve	21%	Ficol 87%
1°3b/F	35	3.6g/4x10 ⁹	+ve	+ve	NA	Ficol 99%
Secondary mice; 1x10 ⁶ 1°3B spleen cells transplanted / mouse.						
2°3a/M	16	2.53g/4x10 ⁹	+ve	+ve	38%	Ficol 92%
2°3b/M	16	0.28g/3.6x10 ⁶	+ve	+ve	29%	Ficol 97%
2°3c/M	15	2.4g/7x10 ⁸	+ve	+ve	36%	Ficol 95%
2°3d/M	16	3.6g/3.22x10 ⁹	+ve	+ve	34%	Ficol 95%
2°3e/M	16	1.3g/6x10 ⁸	+ve	+ve	32%	Ficol 95%
Patient 4; NA						
Primary mice; 2x10 ⁵ cells transplanted / mouse.						
1°4a/F	22	enlarged*/NA	+ve	+ve	NA	Ficol 95%
1°4b/F	20	1.3g/1.4x10 ⁹	+ve	+ve	NA	Ficol 97%
1°4c/F	20	1.3g/9.7x10 ⁸	+ve	+ve	95%	Ficol 96%

Patient 5; CD19 56%, CD10 59%, CD34 62%.						
Primary mouse; 1x10 ⁶ cells transplanted.						
1 ^{5a} /F	53	0.80g/6x10 ⁸	+ve	+ve	NA	Ficol 80%
Transduced with pSLIEW and analysed by in-vivo imaging and histology post-mortem						
Patient 1; 1.5x10⁶ transduced 3[°]1E spleen cells transplanted / mouse						
1a ^{SLIEW} /F	16	0.53g/NA	+ve	NA	NA	Ficol 92%
1b ^{SLIEW} /F	18	0.88g/NA	+ve	NA	NA	Ficol 92%
Patient 2; 1.5x10⁶ transduced 2[°]2E spleen cells transplanted / mouse						
2a ^{SLIEW} /F	16	0.40g/NA	+ve	NA	NA	Ficol 86%
2b ^{SLIEW} /F	14	0.55g/2x10 ⁸	+ve	NA	NA	Ficol 89%
Patient 3; 1.5x10⁶ transduced 2[°]3D spleen cells transplanted / mouse						
3a ^{SLIEW} /F	15	0.23g/NA	+ve	NA	NA	Ficol 85%
3b ^{SLIEW} /F	15	0.27g/NA	+ve	NA	NA	Ficol 94%
Patient 4; 1.5x10⁶ transduced 1[°]4B spleen cells transplanted / mouse						
4a ^{SLIEW} /F	15	0.83g/NA	+ve	NA	NA	Ficol 89%
4b ^{SLIEW} /F	14	0.81g/NA	+ve	NA	NA	Ficol 79%

Ficol indicates that the sample was purified by Ficol gradient separation. * Spleen weight not recorded but splenomegaly noted. ** Tumour load refers to the total number of cells isolated (a variable proportion of cells are lost in the course of purification over Ficol). NA data not available.

Supplementary table 5. Xenograft Immunophenotypic data.

id	%CD19+ve (MFI)		%CD10+ve (MFI)		%CD34+ve (MFI)		%CD38+ve (MFI)	
	BM	spleen	BM	spleen	BM	spleen	BM	spleen
Patient 1; CD19 92%, CD10 94%, CD34 93%.								
primary mice								
1°1a	100 (10920)	100 (11171)	100 (21462)	100 (18458)	52 (5224)	51 (4623)	18 (567)	10 (474)
1°1b	100 (10133)	100 (12845)	99 (9642)	100 (53563)	44 (2940)	78 (12640)	3 (340)	50 (1579)
secondary mice								
2°1a	100 (28751)	100	100 (61831)	100	100 (19668)		97 (4334)	
2°1b	100 (21717)	100 (24860)	100 (59035)	100 (80485)	96 (17696)	97 (20089)	88 (3028)	91 (3234)
tertiary mice								
3°1a	100	100 (21614)	100	100 (51772)		90 (14720)		93 (4281)
3°1b	100	100 (16847)	100	100 (42753)		70 (11325)		72 (3170)
3°1c		100 (18589)		100 (43906)		82 (11666)		82 (3113)
3°1d		100 (16382)		100 (46420)		72 (12212)		75 (3170)
3°1e	100	100 (17125)	100	100 (45972)		69 (11586)		73 (3132)
3°1f		100 (19948)		100 (48138)		77 (12268)		83 (3095)
3°1g	100 (24742)	100 (15819)	100 (68666)	100 (46872)	94 (17696)	89 (12815)	97 (4831)	94 (3847)
Patient 2; CD19 85%, CD10 83%, CD34 80%								
primary mouse								
1°2a	100	100	100	100				
secondary mice								
2°2a	100 (14349)	100 (12815)	100 (51397)	100 (38352)	82 (15065)	84 (12296)	85 (3089)	63 (1881)
2°2b	100	100 (10341)	100	100 (38723)		89 (11020)		39 (1204)
2°2c		100		100				
2°2d		100 (8262)		100 (36547)		88 (10341)		16 (762)
2°2e	100 (9664)	100 (7629)	100 (45750)	100 (30305)	91 (14283)	89 (9513)	29 (1125)	1 (700)
2°2f	100 (11171)	100 (12101)	100 (61831)	100 (54881)	93 (17490)	92 (14652)	55 (1902)	51 (1652)
2°2g	100	100	100	100				
Patient 3; CD19 85%, CD10, 84%, CD34 83%								
primary mice								
1°3a	100	100	100	100				
1°3b		100		100				
Secondary mice								
2°3a	100 (21110)	100 (26956)	100(143642)	100(124849)	84 (29236)	81 (26384)	19 (1784)	6 (1320)
2°3b	100	100 (22448)	100	100(130499)		56 (25038)		1 (1188)
2°3c	100	100 (20137)	100	100(127329)		82 (27739)		3 (1290)
2°3d	100	100 (24161)	100	100(130499)		78 (25038)		3 (1188)
2°3e	100	100 (19807)	100	100(120329)		66 (24334)		1 (1127)
Patient 4;								
Primary mice								
1°4a		100 (17367)		100 (30743)		60 (7817)		19 (807)
1°4b		100 (17820)		100 (54747)		80 (18853)		66 (2428)
1°4c	100	100 (18941)	100	100 (37984)		35 (8027)		88 (3532)

Patient 5; CD19 56%, CD10 59%, CD34 62%.								
Primary mouse								
1 ^{5a}	100	100	100	100				
Transduced with pSLEW and analysed by in-vivo imaging and histology post-mortem								
Patient 1								
1a ^{SLEW}		100		100				
1b ^{SLEW}		100 (16926)		100 (57616)		71 (13235)		86 (3400)
Patient 2								
2a ^{SLEW}		100		100				
2b ^{SLEW}		100		100				
Patient 3								
3a ^{SLEW}		100 (18720)		100(145780)		48 (27345)		0 (1744)
3b ^{SLEW}		100		100				
Patient 4								
4a ^{SLEW}		100 (15709)		100 (36635)		58 (9156)		77 (3046)
4b ^{SLEW}		100		100				

Mean fluorescence intensity (MFI). Gray boxes indicate that no sample was available for analysis.

Supplementary table 6. Bone marrow histology of additional xenografts.

Xenograft ID	Genetic sub-type	Sample	Morphology type*
1°5Ra	iAMP21	femur/sternum	A
1°5Rb	iAMP21	femur/sternum	A/B
1°13a	iAMP21	tibia	A
1°13b	iAMP21	tibia/sternum	A
1°14a	iAMP21	tibia/sternum	A
1°14b	iAMP21	tibia/sternum	A
1°14c	iAMP21	tibia	A
1°15a	iAMP21	tibia/sternum	WT/A
1°15b	iAMP21	tibia/sternum	A
1°16a	iAMP21	humerus/sternum	WT/A
1°16b	iAMP21	humerus/sternum	WT/A
2°17a	ETV6-RUNX1	tibia	A
1°18a	Hyperdiploid	forelimb/sternum	A/B

*WT (wild type morphology similar to control NSG mice), A and B (as defined in the main text and shown in figures 2, and Supplementary figures 3 and 7).

Patient 2 concordant CNA

2° xenografts

Chr	Abnormality	genome position	patient	a	b	c	d	e	f	genes
3	del (CN 1)	35528000-35684000	Y	Y	Y	Y	Y	Y	Y	ARPP21 (exons1&2)
6	del (CN 1)	46699000-47018000	Y	Y	Y	Y	Y	Y	Y	PLA2G7, LOC100287718, MEP1A, GPR116, GPR110
7	del (CN 1)	50150000-51210000	Y	Y	Y	Y	Y	Y	Y	C7orf72, IKZF1, FIGNL1, DDC, GRB10, COBL
7	del (CN 1)	109732000-158646480	Y	Y	Y	Y	Y	Y	Y	many
8	del (CN 1)	53567000-53596000	Y	Y	Y	Y	Y	Y	Y	RB1CC1 (exons 9-20)
9	del (CN 1)	0-39500000	Y	Y	Y	Y	Y	Y	Y	many
9	del (CN 0)	20365000-22404000	Y	Y	Y	Y	Y	Y	Y	32 genes MLLT3-CDKN2B-AS1
9	amp (CN 3)	70950000-141067840	Y	Y	Y	Y	Y	Y	Y	many
11	del (CN 1)	63950000-64000000	Y	Y	Y	Y	Y	Y	Y	STIP1, FERMT3, TRPT1, NUDT22, DNAJC4, VEGFB
12	del (CN 1)	11846000-11930000	Y	Y	Y	Y	Y	Y	Y	ETV6 (ex 2)
13	amp (CN 3)	67315000-115150780	Y	Y	Y	Y	Y	Y	Y	many
16	del (CN 1)	3781000-3824000	Y	Y	Y	Y	Y	Y	Y	CREBBP (ex 1-19)
20	del (CN 1)	56168000-56690000	Y	Y	Y	Y	Y	Y	Y	ZBP1, PMEPA1, MIR4532
22	del (CN 1)	22320000-22540000	Y	Y	Y	Y	Y	Y	Y	TOP3B
X	WCG		Y	Y	Y	Y	Y	Y	Y	

Patient 2 discordant CNA

2	del (CN 1)	74000000-86000000	N	N	N	S	N	N	N	Many TPRKB-ST3GAL5
12	trisomy		Y	N	N	N	N	N	N	
X	iso(p)		N	N	N	S	Y	N	N	many
X	del (CN 1)	47248000-47342000	N	N	Y	S	S	S	S	ZNF157, ZNF41

Patient 3 concordant CNA

1° 2° xenografts

Chr	Abnormality	genomic position	patient	a	b	a	b	c	d	e	genes
4	amp (CN 3)	70125000-70238000	Y	Y	Y	Y	Y	Y	Y	Y	UGT2B28
5	trisomy		Y	Y	Y	Y	Y	Y	Y	Y	
10	trisomy		Y	Y	Y	Y	Y	Y	Y	Y	
12	del (CN 1)	104860000-105042000	Y	Y	Y	Y	Y	Y	Y	Y	CHST11 (ex 2&3)
14	trisomy		Y	Y	Y	Y	Y	Y	Y	Y	
17	trisomy		Y	Y	Y	Y	Y	Y	Y	Y	
17	del (CN 1)	62590000-62665000	Y	Y	Y	Y	Y	Y	Y	Y	SMURF2 (ex 15-18)
X	del (CN 1)	1380000-1604000	Y	Y	Y	Y	Y	Y	Y	Y	CSF2RA, IL3RA, SLC25A6, ASMTL-AS1, ASMTL, P2RY8(UTR).

Patient 3 discordant CNA

9	trisomy		Y	Y	N	N	N	N	N	N	
12	del (CN 1)	0-24500000	S	S	N	N	N	N	N	N	
12	del (CN 1)	11950000-32460000	N	N	S	N	N	N	N	N	ETV6 (ex 3-7) many genes BICD1 (exon 1-4)
X	trisomy		Y	S	Y	Y	S	Y	S	S	

patient 4 concordant CNA

Chr	Abnormality	genomic position	1° xenografts		genes in region
			1	2	
1	complex	89800000-121500000	Y	Y	many
1	del (CN 0)	152550000-152590000	Y	Y	LCE3, LCE3B, LCE3A
1	del (CN 1)	196720000-196800000	Y	Y	CFHR3, CFHR1
2	del (CN 1)	184500000-184600000	Y	Y	ZNF804A
5	del (CN 1)	142674000-142750000	Y	y	NR3C1
5	del (CN 0)	142674000-142724350	Y	y	NR3C1
9	del (CN 1)	0-34150000	Y	y	many including CDKN1A/B
9	del (CN 0)	21954000-22119000	y	y	CDKN1A, CDKN1B, CDKN1B-AS1
9	del (CN 1)	37000000-37350000	Y	Y	PAX5, ZCCHC7
10	del (CN 0)	98350000-98700000	Y	Y	PIK3AP1, LCOR
11	del (CN1)	82000000-134963460	Y	Y	many
12	del (CN 1)	11800000-12000000	Y	Y	ETV6 intragenic
12	del (CN 0)	111760000-112060000	Y	Y	CUX2, FAM109A, SH2B3, ATXN2
12	del (CN 1)	133350000-133800000	Y	Y	COLGA3, CHFR, ZNF605, ZNF26, ZNF84, ZNF140, ZNF10, ZNF268, ANHX
13	del (CN 1)	44600000-45050000	Y	Y	SERP2
20	del (CN 1)	1500000-1630000	Y	Y	SIRPD, SIRPB1, SIRPG

Patient 4 discordant CNA

4	del (CN 1)	174060000-174260000	Y	N	GALNT7, HMGB2
4	amp (CN2)	69350000-69500000	N	Y	UGT2B17
10	del (CN 1)	90000000-135534000	Y	Y	many
10	del (CN 1))	80800000-126400000	N	N	many
10	del (CN 0)	98015000-98060000	N	Y	BLNK
14	amp (CN 3)	36900000-43900000	Y	N	13 genes SLC25A21- LRFN5
14	del (CN 1)	43900000-107349520	Y	N	many
16	del (CN 1)	3770000-3920000	Y	N	CREBBP
17	amp (CN 1)	25300000-27450000	N	N	many
17	amp (CN 2)	25920000-26300000	Y	Y	many
17	amp (CN 1)	25300000-25920000	Y	Y	many
22	del (CN 1)	37630000-37740000	N	N	RAC2, CYTH4

Patient 5 concordant CNA

Chr	Abnormality	genomic position	patient		1° xenograft	genes
			presentation	relapse	a	
2	del (CN 1)	63776000-75095000	y	Y	Y	many
4	del (CN 1)	71760000-71900000	y	Y	Y	MOB1B, DCK
6	del (CN 1)	26126000-26260000	y	Y	Y	16 genes HIST1H1E- HIST1H2BH

Patient 5 discordant CNA

1	del (CN 1)	234612000-235540000	N	N	S	8 genes TARBP1- ARID4B,
2	del (CN 1)	2322000-8874000	S	N	Y	LOC100506274, LOC339788, LINC00299, ID2, KIDINS220 (ex 1)
3	del (CN 1)	114080000-114680000	S	N	Y	ZBTB20
3	del (CN 1)	45900000-48250000	S	Y	N	37 genes CCR9-CAMP
5	del (CN 1)	158088000-158149000	N	N	S	EBF1 exons 1-5
5	del (CN 1)	158380000-158580000	N	Y	N	EBF1 exons 10-16
12	CN-LOH	53500000-133721800	Y	Y	N	many
12	del (CN 1)	111050000-112135000	S	N	Y	12 genes TCTN1- ACAD10

Supplementary Table 8. Regions of chromosome 21 copy number change that occurred in xenografts from patient 1.

start	end	size	CN change
0	16446092	16446092	0
16446092	17302313	856221	1
17381183	17697572	316389	-2
17697723	18163458	465735	-1
18163544	18174691	11147	0
18177172	20521089	2343917	-1
20521648	21760268	1238620	0
21760283	22125481	365198	-2
22125690	22517120	391430	0
22517189	23343710	826521	-2
23345771	26533474	3187703	0
26533786	28305871	1772085	-1
28306308	29236061	929753	-2
29243377	31443709	2200332	-1
31447334	31680485	233151	0
31683535	33949423	2265888	-1
33949543	48096945	14147402	0

Supplementary Table 9. MLPA values for patients and their xenografts. A score of 1 indicates normal copy number. Examples with clear evidence for CN changes between samples are highlighted (loss by shades of red and gain by shades of green).

Target	Patient 1		
	patient	xenografts	
		2°1b	3°1g
01a_EBF1_ex16	1.035	0.855	1.142
01b_EBF1_ex14	1.086	1.114	0.952
01c_EBF1_ex10	1	0.974	1.16
01d_EBF1_ex1	0.965	0.958	1.127
02a_IKZF1_ex1	0.588	0.499	0.596
02b_IKZF1_ex2	0.649	0.481	0.56
02c_IKZF1_ex3	0.616	0.451	0.598
02d_IKZF1_ex4	0.583	0.454	0.603
02e_IKZF1_ex5	0.639	0.435	0.567
02f_IKZF1_ex6	0.609	0.566	0.529
02g_IKZF1_ex7	0.636	0.511	0.597
02h_IKZF1_ex8	0.55	0.49	0.622
03a_JAK2_ex23		0.844	0.825
03b_CDKN2A_ex5	0.936	0.987	0
03c_CDKN2A_ex2a	1.022	0.897	0
03d_CDKN2B_ex2	1.021	0.919	0
04a_PAX5_ex10	1.032	0.97	1.255
04b_PAX5_ex8	0.942	0.828	1.236
04c_PAX5_ex7		0.966	0.994
04d_PAX5_ex6	1.015	0.974	1.183
04e_PAX5_ex5	0.981	1.086	0.996
04f_PAX5_ex2	1.149	0.795	1.171
04g_PAX5_ex1	0.981	0.938	1.149
05a_ETV6_ex1A	0.97	1.048	0.969
05b_ETV6_ex1B	1.003	1.1	0.948
05c_ETV6_ex2	0.201	0	0.527
05d_ETV6_ex3	0.401	0.511	0.473
05e_ETV6_ex5	0.616	9	0.627
05f_ETV6_ex8	0.986	0.945	1.122
06a_BTG1-AREA1	0.972	0.913	1.043
06b_BTG1-AREA2	0.893	0.919	1.106
06c_BTG1_ex2	1.038	0.967	1.14
06d_BTG1_ex1	1.06	0.815	1.262
07a_RB1_ex6	0.955	0.874	1.137
07b_RB1_ex14	1.015	94	0.967
07c_RB1_ex19	0.117	0	0
07d_RB1_ex24	0.118	0	0
07e_RB1_ex26	0.095	0	0
08a_SHOX_area	1.01	0.918	0.995
08b_CRLF2_ex4	0.997	0.942	1.09
08c_CSF2RA_ex10	1.043	0.993	0.924
08d_IL3RA_ex1	0.98	1.038	0.852
08e_P2RY8_ex2	0.987	0.943	1.106
08f_ZFY_ex4	0	-1	-1

Patient 2						
Target	patient	secondary xenografts				
		2°2c	2°2d	2°2b	2°2e	2°2f
01a_EBF1_ex16	0.975	0.965	0.918	0.945	1.054	1.019
01b_EBF1_ex14	0.948	0.949	1.025	0.953	0.84	0.901
01c_EBF1_ex10	0.965	0.994	1.06	1.061	1.083	1.083
01d_EBF1_ex1	0.898	1.051	1.067	0.998	1.157	1.078
02a_IKZF1_ex1	0.485	0.541	0.602	0.579	0.538	0.551
02b_IKZF1_ex2	0.539	0.53	0.583	0.536	0.572	0.543
02c_IKZF1_ex3	0.547	0.535	0.541	0.555	0.579	0.579
02d_IKZF1_ex4	0.55	0.539	0.599	0.59	0.598	0.622
02e_IKZF1_ex5	0.544	0.534	0.544	0.526	0.574	0.559
02f_IKZF1_ex6	0.575	0.494	0.497	0.494	0.447	0.53
02g_IKZF1_ex7	0.483	0.599	0.665	0.598	0.61	0.588
02h_IKZF1_ex8	0.509	0.611	0.648	0.602	0.645	0.635
03a_JAK2_ex23	0.565	0.426	0.432	0.409	0.368	0.396
03b_CDKN2A_ex5	0	0	0	0	0	0
03c_CDKN2A_ex2a	0	0	0	0	0	0
03d_CDKN2B_ex2	0	0	0	0	0	0
04a_PAX5_ex10	0.512	0.591	0.622	0.587	0.669	0.625
04b_PAX5_ex8	0.5	0.732	0.823	0.862	0.703	0.637
04c_PAX5_ex7	0.552	0.659	0.72	0.677	0.497	0.482
04d_PAX5_ex6	0.512	0.592	0.662	0.633	0.629	0.653
04e_PAX5_ex5	0.56	0.545	0.593	0.54	0.451	0.491
04f_PAX5_ex2	0.508	0.548	0.616	0.647	0.605	0.591
04g_PAX5_ex1	0.516	0.556	0.595	0.639	0.624	0.632
05a_ETV6_ex1A	1.344	1.016	1.047	1.027	0.942	0.919
05b_ETV6_ex1B	1.307	0.939	0.948	0.97	0.875	0.891
05c_ETV6_ex2	0.596	0.522	0.532	0.506	0.456	0.476
05d_ETV6_ex3	1.378	0.915	0.921	0.89	0.856	0.924
05e_ETV6_ex5	1.39	1.069	1.047	1.076	1.146	1.123
05f_ETV6_ex8	1.283	1.07	1.074	1.068	1.126	1.101
06a_BTG1-AREA1	1.215	0.945	0.973	0.924	0.997	0.95
06b_BTG1-AREA2	1.247	1.02	1.039	1.021	1.043	1.04
06c_BTG1_ex2	1.258	1.078	1.093	1.033	1.138	1.104
06d_BTG1_ex1	1.141	1.229	1.391	1.395	1.256	1.307
07a_RB1_ex6	0.909	1.013	1.06	0.991	1.087	1.077
07b_RB1_ex14	0.984	0.962	0.998	0.939	0.894	0.924
07c_RB1_ex19	0.93	1.031	1.094	1.012	0.919	0.926
07d_RB1_ex24	1.004	1.048	1.023	1.029	0.85	0.955
07e_RB1_ex26	0.998	0.954	0.876	0.88	0.83	0.877
08a_SHOX_area	1.404	1.315	1.26	1.332	1.651	1.347
08b_CRLF2_ex4	1.446	1.34	1.486	1.343	1.46	1.536
08c-CSF2RA_ex10	1.496	1.268	1.205	1.111	1.351	1.221
08d_IL3RA_ex1	1.353	1.384	1.506	1.433	1.328	1.232
08e_P2RY8_ex2	1.252	1.52	1.717	1.657	1.893	1.637
08f_ZFY_ex4	1000	1000	1000	1000	1000	1000

Patient 3							
Target	Patient	xenografts					
		1°3b	2°3c	2°3a	2°3e	2°3b	2°3d
01a_EBF1_ex16	1.356	1.432	1.506	1.529	1.449	1.553	1.507
01b_EBF1_ex14	1.306	1.403	1.319	1.298	1.323	1.319	1.423
01c_EBF1_ex10	1.405	1.223	1.571	1.596	1.522	1.621	1.512
01d_EBF1_ex1	1.363	1.511	1.521	1.621	1.574	1.56	1.429
02a_IKZF1_ex1	1.01	1.047	1.051	1.059	1.041	1.038	0.987
02b_IKZF1_ex2	0.964	0.969	1.022	1.083	1.051	1.037	0.999
02c_IKZF1_ex3	0.978	1.042	1.053	1.09	1.096	1.089	1.063
02d_IKZF1_ex4	0.949	1.033	1.034	1.17	1.098	1.14	1.066
02e_IKZF1_ex5	1	0.95	1.019	1.063	1.054	1.048	0.994
02f_IKZF1_ex6	1.109	0.901	0.891	0.915	0.916	0.994	1.018
02g_IKZF1_ex7	0.941	1.198	1.143	1.164	1.168	1.102	1.077
02h_IKZF1_ex8	1.037	1.183	1.153	1.239	1.213	1.185	1.094
03a_JAK2_ex23		0.722	0.652	0.676	0.719	0.783	0.836
03b_CDKN2A_ex5	1.227	1.011	1.054	1.154	1.116	1.104	1.009
03c_CDKN2A_ex2a	1.348	1.171	1.018	1.037	1.033	1.022	0.964
03d_CDKN2B_ex2	1.215	1.128	1.076	1.142	1.116	1.074	1.034
04a_PAX5_ex10	1.096	1.275	1.214	1.239	1.185	1.164	1.121
04b_PAX5_ex8	1.334	1.676	1.42	1.156	1.213	1.138	1.242
04c_PAX5_ex7		1.391	1.084	0.848	0.919	0.909	1.095
04d_PAX5_ex6	1.231	0.938	0.983	1.189	1.162	1.19	1.113
04e_PAX5_ex5	1.309	0.798	0.729	0.913	0.97	0.923	0.973
04f_PAX5_ex2	1.213	1.063	1.008	1.106	1.105	1.158	1.05
04g_PAX5_ex1	1.207	1.06	1.089	1.145	1.077	1.136	1.046
05a_ETV6_ex1A	0.838	1.009	0.912	0.85	0.915	0.91	0.939
05b_ETV6_ex1B	0.843	0.926	0.882	0.826	0.855	0.877	0.875
05c_ETV6_ex2	0.856	1.001	0.942	0.868	0.883	0.909	0.944
05d_ETV6_ex3	0.868	0.541	0.737	0.758	0.791	0.792	0.864
05e_ETV6_ex5	0.86	0.709	1.106	1.017	1.083	1.02	1.04
05f_ETV6_ex8	0.85	0.68	1.028	0.964	1.008	1.007	0.974
06a_BTG1-AREA1	1.003	0.933	0.941	0.95	0.948	0.977	0.922
06b_BTG1-AREA2	1.136	1.031	0.989	1.013	0.988	1.064	0.976
06c_BTG1_ex2	0.91	1.085	1.098	1.081	1.065	1.132	1.045
06d_BTG1_ex1	0.953	1.322	1.114	1.295	1.231	1.304	1.086
07a_RB1_ex6	1.079	1.013	1.026	1.093	0.992	1.049	0.985
07b_RB1_ex14	0.998	0.938	0.871	0.817	0.841	0.863	0.917
07c_RB1_ex19	0.875	1.016	0.929	0.914	0.911	0.922	0.962
07d_RB1_ex24	0.926	0.987	0.918	0.953	0.91	0.954	0.978
07e_RB1_ex26	0.933	0.885	0.855	0.884	0.835	0.913	0.958
08a_SHOX_area	1.305	1.204	1.202	1.374	1.186	1.18	1.279
08b_CRLF2_ex4	1.325	1.191	1.445	1.454	1.209	1.239	1.437
08c-CSF2RA_ex10	0.579	0.451	0.35	0.379	0.216	0.195	0.408
08d_IL3RA_ex1	0.583	0.412	0.301	0.377	0.24	0.199	0.402
08e_P2RY8_ex2		0.562	0.453	0.514	0.282	0.237	0.441
08f_ZFY_ex4		-1	-1	-1	-1	-1	-1

Patient 5		
Target	patient	primary xenograft 1°5a
01a_EBF1_ex16	0.777	0.536
01b_EBF1_ex14	0.771	0.554
01c_EBF1_ex10	0.928	1.006
01d_EBF1_ex1	0.865	0.988
02a_IKZF1_ex1	0.97	1.025
02b_IKZF1_ex2	1.005	1.004
02c_IKZF1_ex3	0.956	1.003
02d_IKZF1_ex4	0.966	1.028
02e_IKZF1_ex5	1	1.011
02f_IKZF1_ex6	1.09	0.994
02g_IKZF1_ex7	0.905	0.975
02h_IKZF1_ex8	0.964	1.013
03a_JAK2_ex23		0.976
03b_CDKN2A_ex5	0.998	0.564
03c_CDKN2A_ex2a	1.004	0.542
03d_CDKN2B_ex2	1.017	0.979
04a_PAX5_ex10	0.904	1.032
04b_PAX5_ex8	0.971	0.93
04c_PAX5_ex7	1.143	0.948
04d_PAX5_ex6	0.98	1.05
04e_PAX5_ex5	1.013	1.018
04f_PAX5_ex2	1	1.062
04g_PAX5_ex1	0.988	1.042
05a_ETV6_ex1A	1.025	0.995
05b_ETV6_ex1B	1	1.002
05c_ETV6_ex2	1.019	1.014
05d_ETV6_ex3	1	1.035
05e_ETV6_ex5	1	1.033
05f_ETV6_ex8	0.991	1.02
06a_BTG1-AREA1	1.022	0.986
06b_BTG1-AREA2	1.031	0.938
06c_BTG1_ex2	0.983	1.001
06d_BTG1_ex1	1.011	0.995
07a_RB1_ex6	1.022	1.022
07b_RB1_ex14	1.039	1.031
07c_RB1_ex19	1.01	0.906
07d_RB1_ex24	1.2	0.949
07e_RB1_ex26	0.982	0.914
08a_SHOX_area	0.984	1.019
08b_CRLF2_ex4	1.038	1.041
08c_CSF2RA_ex10	1.008	1.018
08d_IL3RA_ex1	1	1.031
08e_P2RY8_ex2	0.979	1.04
08f_ZFY_ex4	0	-1

References for supplementary methods.

1. Bomken S, Buechler L, Rehe K, et al. Lentiviral marking of patient-derived acute lymphoblastic leukaemic cells allows in vivo tracking of disease progression. *Leukemia*. 2013;27(3):718-721.
2. Williams MT, Yousafzai YM, Elder A, et al. The ability to cross the blood-cerebrospinal fluid barrier is a generic property of acute lymphoblastic leukemia blasts. *Blood*. 2016;127(16):1998-2006.
3. Ryan SL, Matheson E, Grossmann V, et al. The role of the RAS pathway in iAMP21-ALL. *Leukemia*. 2016; 30:1824-1831.
4. Conway T, Wazny J, Bromage A, et al. Xenome--a tool for classifying reads from xenograft samples. *Bioinformatics*. 2012;28(12):i172-178.
5. Li H, Durbin R. Fast and accurate short read alignment with Burrows-Wheeler transform. *Bioinformatics*. 2009;25(14):1754-1760.
6. Li H, Durbin R. Fast and accurate long-read alignment with Burrows-Wheeler transform. *Bioinformatics*. 2010;26(5):589-595.
7. Cibulskis K, Lawrence MS, Carter SL, et al. Sensitive detection of somatic point mutations in impure and heterogeneous cancer samples. *Nat Biotechnol*. 2013;31(3):213-219.
8. DePristo MA, Banks E, Poplin R, et al. A framework for variation discovery and genotyping using next-generation DNA sequencing data. *Nat Genet*. 2011;43(5):491-498.
9. Van der Auwera GA, Carneiro MO, Levy-Moonshine A, et al. From FastQ data to high confidence variant calls: the Genome Analysis Toolkit best practices pipeline. *Curr Protoc Bioinformatics*. 2013;43:11.10. 1-33.
10. McLaren W, Pritchard B, Rios D, Chen Y, Flicek P, Cunningham F. Deriving the consequences of genomic variants with the Ensembl API and SNP Effect Predictor. *Bioinformatics*. 2010;26(16):2069-70.
11. Robinson JT, Thorvaldsdottir H, Winckler W, et al. Integrative genomics viewer. *Nat Biotechnol*. 2011;29(1):24-6.
12. Harrison CJ, Moorman AV, Schwab C, et al. An international study of intrachromosomal amplification of chromosome 21 (iAMP21): cytogenetic characterization and outcome. *Leukemia*. 2014;28(5): 1015-1021.

